Available online at www.sciencedirect.com
SCIENCE DIRECT®
Journal of Nuclear Materials 336 (2005) 267–278
journal of nuclear materials
www.elsevier.com/locate/jnucmat

The relationship between hardness and yield stress in irradiated austenitic and ferritic steels

Jeremy T. Busby *, Mark C. Hash, Gary S. Was

2355 Bonisteel Blvd., 2937 Cooley Building, University of Michigan, Ann Arbor, MI 48109-2104, USA

Received 4 February 2004; accepted 27 September 2004

Abstract

Microhardness testing is an efficient means of assessing the mechanical properties of many materials, and is especially convenient for irradiated samples because of the small sampling volume requirement. This paper provides correlations between hardness and yield stress for both irradiated austenitic and ferritic steels by combining existing data in the open literature. For austenitic stainless steels, seven data sets were assembled and the change in yield stress was determined to simply be the change in hardness times a factor of 3.03. For the pressure vessels steels, five studies containing both hardness and yield stress data were combined. In ferritic steels, the correlation factor between change in yield stress and change in hardness was found to be 3.06. The similarity in correlation factors for austenitic and ferritic steels is consistent with previous theoretical and experimental results.

1. Introduction

Radiation-induced microstructure and hardening have been studied extensively in a number of alloy systems and under various irradiation conditions [1,2]. The mechanical properties of irradiated alloys change significantly during exposure [3]. Two broad categories of mechanical property changes are of critical importance to reactor core internals and pressure vessel steels: radiation-induced hardening, usually referring to an increase in yield stress and ultimate tensile stress as a function of irradiation dose or temperature, and radiation-induced embrittlement or a reduction in plastic or ductile deformation occurring before failure. Measurement and prediction of hardening and embrittlement in austenitic and ferritic alloys is important for accurate prediction of component lifetime.

The direct measurement of yield strength of irradiated materials is clearly the most desirable way to monitor irradiation-induced hardening. However, the handling and testing of samples with high residual radioactivity is more difficult as the testing must be performed in hot cells. As such, the yield stress of a neutron-irradiated alloy can be difficult to determine when compared to unirradiated materials. Correlations have been developed which allow calculation of expected yield strengths from measured microstructural features such as dislocation loops and voids. However, the existing database of radiation-induced microstructure is also relatively sparse and the correlations are not yet widely developed for all alloys of interest.

Microhardness testing provides an alternative means of assessing changes in mechanical properties. Vickers

* Corresponding author. Tel.: +1 734 764 5225; fax: +1 734 763 4540.
E-mail address: jbusby@engin.umich.edu (J.T. Busby).

0022-3115/$ - see front matter
doi:10.1016/j.jnucmat.2004.09.024

hardness testing can be done quickly and efficiently, without need for a large volume of sample material, an important consideration for highly radioactive neutron-irradiated materials. Microhardness testing is also quasi-non-destructive leaving much of the sample available for other tests. Microhardness testing also provides a means for assessing radiation-induced hardening in ion-irradiated alloys. Ion irradiation has been shown to be a useful tool in assessing irradiation-induced changes (hardening, microstructure, radiation-induced segregation, and even irradiation-assisted stress corrosion cracking) [4] without the very long irradiation times and high levels of residual radioactivity associated with neutron irradiation. While the yield stress of the thin damaged layer in an ion-irradiated sample cannot be measured directly, microhardness tests can easily be with high precision. Correlations have been developed which allow calculation of expected yield strengths from measured hardness [5].

The purpose of this work is to determine correlations between hardness and yield stress for irradiated austenitic and ferritic steels. The physical relationship between hardness and yield stress will be examined for both austenitic and ferritic alloys relevant to nuclear power reactors. For each system, a brief review of existing hardness/yield stress correlations and the available data sets is first provided. A relevant correlation is then developed for each alloy system.

2. Physical relationship between hardness and yield stress

While a correlation between two values is useful by itself, the underlying relationship between those parameters is more meaningful. In this section, the physical relationship between hardness and yield stress are examined. The analysis presented here is oversimplified, although more detailed studies are available.

As originally described by Tabor [5], the indentations made during hardness tests are discernible as permanent impressions in the metal, so the indentation must be primarily a measure of the plastic properties of the metal. While it is true that some change in shape and size occurs when the indenter is removed, the overriding effect is the plastic flow of the metal around the indenter tip, implying that the mean pressure over the indenter is connected to the plastic rather than elastic properties of the metal. Tabor [5] shows that this is indeed the case for a variety of different hardness and scratch tests, based on the work of Prandtl [6] and Hencky [7] and that hardness measurement can also be used as a measure of the yield stress of the metal.

As Tabor originally described, during indentation, stress is applied to the metal surface through the indenter tip. However, since the tip surface is not parallel to the sample surface, the stress state during indentation is not simple compressive. Instead, the stresses must be examined in two dimensions (along and perpendicular to the axis of the indenter tip). Plastic deformation during indentation occurs when the Huber-Mises criterion is satisfied, which in the two-dimensional case, occurs when the maximum shear stress reaches a critical value, k:

$$2k = 1.15\sigma_y, \tag{1}$$

where σ_y is the yield stress.

The pyramidal shape of the indenter tip can be treated as a wedge during indentation. The pattern of plastic flow around the indenter tip during indentation can be determined using the Prandtl solution [6]. The flow pattern is shown schematically in Fig. 1 for a Vickers indentation. The pressure normal to the surface of the indenter tip can be calculated as

$$P = 2k(1 + \pi/2). \tag{2}$$

Eqs. (1) and (2) can be combined to yield:

$$P = 2k(1 + \pi/2) = 1.15\sigma_y(1 + \pi/2) = 2.96\sigma_y. \tag{3}$$

For a Vickers indenter:

$$H_v \equiv \frac{\text{Load}}{\text{Contact Area}} = 0.927P, \tag{4}$$

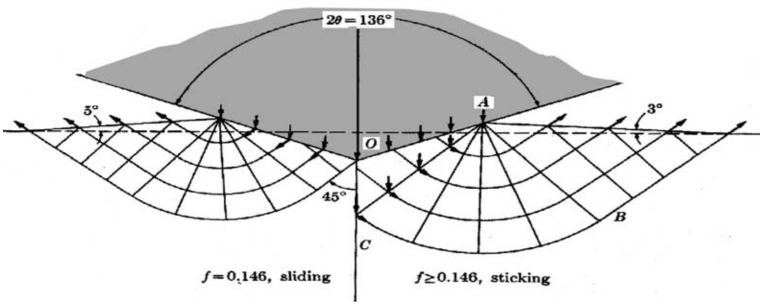

Fig. 1. Flow pattern during Vicker's indentation of a material [5].

where 0.927 is the ratio of the area of the base of the pyramid (the projected area) to the area of the sides of the pyramid (contact area). Combining Eqs. (3) and (4) gives,

$$H_v = 0.927P = 0.927x2.96\sigma_y = 2.74\sigma_y. \quad (5)$$

Reversing this relationship:

$$\sigma_y = 0.364H_v, \quad (6a)$$

with σ_y and H_v in kg/mm^2. Alternatively,

$$\sigma_y = 3.55H_v, \quad (6b)$$

with σ_y in MPa and H_v in kg/mm^2.

Tabor found the same result experimentally for a variety of materials (aluminum, copper, and mild steel). More recently, Larsson [8] studied indentation tests both theoretically and numerically. Specifically, he used finite element analysis to examine elastic–plastic material behavior under sharp contact situations (nano-indenters, Vickers or cone indenters, or even gear contact). Larsson's finite element results were in good agreement with the results of Tabor, validating the assertion that yield stress can, indeed, be determined from Vickers hardness measurements.

3. Austenitic stainless steels

While theoretical calculations are valuable as a guide, correlations based upon experimental results are required for practical application of microhardness indentation as a substitute for yield strength measurement. Experimental data sets from the open literature and existing hardness–yield stress correlations are reviewed in this section. Data from seven different studies (spanning 50 alloys and 133 data points) have been combined to develop a new correlation between hardness and yield stress based on the entire available data set.

3.1. Existing correlations and data

Higgy and Hammad [9] measured the effects of low-temperature (<100 °C) fast neutron irradiation on 304, 316, and 347 SS. They determined the tensile and hardness properties over a range of doses. This data set is shown in Fig. 2(a). For each alloy, the yield stress follows a linear relationship with hardness. It is important to note, however, that the dose range for this study is relatively low, with the highest dose achieved being only 0.2 dpa.

Higgy and Hammad empirically verified that the yield stress and hardness follow a linear relationship of the form

$$\Delta H_v = K\Delta\sigma_y, \quad (7)$$

where both $\Delta\sigma_y$ and ΔH_v are expressed in units of kg/mm^2. The constant K was determined by a linear regression through data spanning a range of hardness and yield stress values. For 304 SS, $K = 2.82$ and for 316 SS and 347 SS, $K = 3.0$. Note that while the form of Eq. (7) is slightly different from that formulated by Tabor in Eq. (6), the constants are very similar in magnitude. Indeed, the values determined by Higgy and Hammad are quite close to those predicted by Tabor.

While Higgy and Hammad's correlation is useful, a correlation based on data from conditions more relevant to LWR core components is desirable. Kodama et al. [10] measured the yield stress and hardness of a series of 23 different 304, 316, and 347 stainless steel alloys following neutron irradiation at 288 °C to doses of 2.9 and 5.0 dpa. The yield stress was measured at elevated temperature (288 °C) in air, while hardness was performed at room temperature. The data set is shown in Fig. 2(b) and exhibits significantly more scatter than that of Higgy and Hammad, which could be the result of the large number of alloys (23) studied. Further, the yield stress results from Kodama relied on only a single tensile sample, while those of Higgy and Hammad are the average of three specimens. Nonetheless, the Kodama data is generated from conditions most relevant to LWR core materials.

Fukuya et al. [11] reported both hardness and yield stress measurements on another 16 stainless steel alloys (304, 316, and 347) neutron-irradiated at 288 °C to ~3.0 dpa. As in Kodama's study, yield stress was measured in air at 288 °C while hardness was performed at room temperature. This experimental data set is illustrated in Fig. 2(c). The data scatter is similar to that for Kodama's data in Fig. 2(b), likely the result of testing only a single tensile specimen on 16 different alloys.

Furutani et al. [12] measured the mechanical properties of a cold-worked 316 stainless steel after irradiation to 5×10^{26} n/m^2 ($E > 0.1$ MeV) at 310 °C (about 25 dpa). The tensile properties were measured at elevated temperature (320 °C) and hardness was measured at room temperature. The data from Furutani et al. is shown in Fig. 2(d).

Allen et al. [13] determined the hardness and yield stress from a section of a "hex can" taken from EBR-II and irradiated at ~370 °C to doses of 1, 20, and 30 dpa The tensile properties and hardness were determined at room temperature. The data from Allen et al. is shown in Fig. 2(e).

Bruemmer et al. [14], used a subset of the data of Kodama (as presented by Suzuki [15]) to create a second correlation. This data set also follows a linear relationship and was fit as

$$\sigma_y = 2.5(H_v - 68), \quad (8)$$

where σ_y is in MPa and H_v is in kg/mm^2. Bruemmer et al. [14] also measured the uniaxial yield stress and Vickers hardness in a cold-worked 316 stainless steel

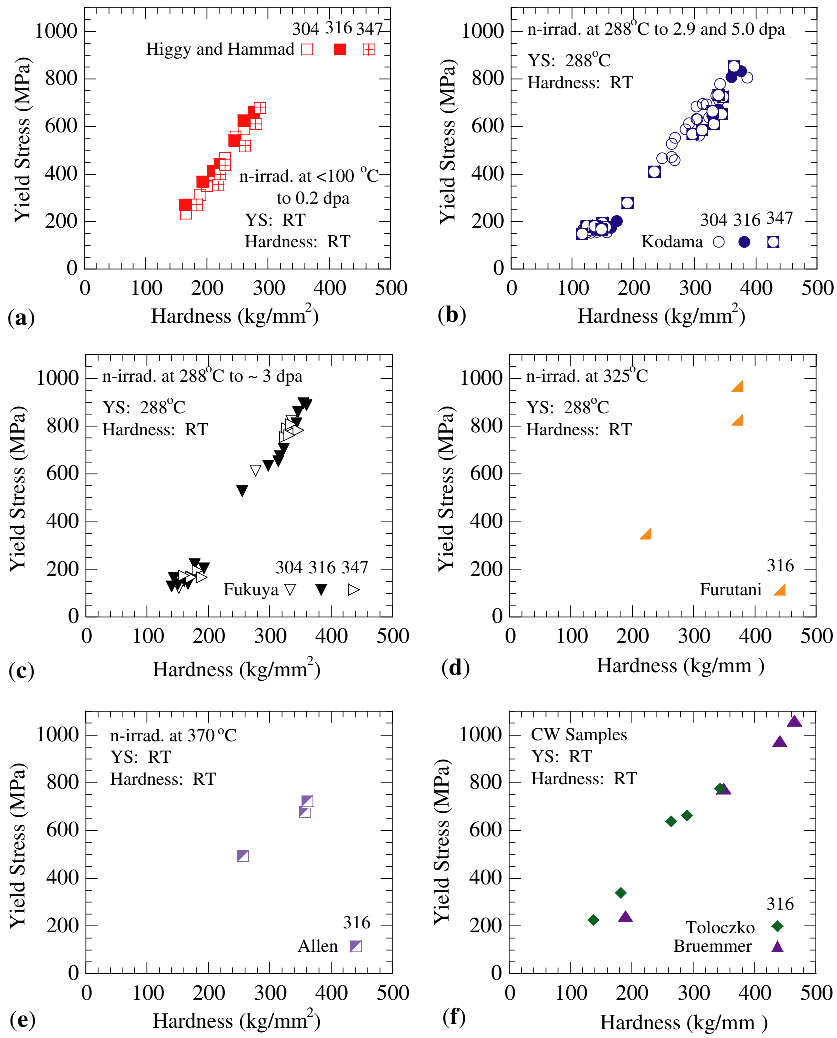

Fig. 2. Available experimental data comparing yield stress and hardness in austenitic stainless steels. Data taken from (a) Higgy and Hammad [9], (b) Kodama et al. [10], (c) Fukuya et al. [11], (d) Furutani et al. [12], (e) Allen et al. [13], and (f) Toloczko et al. [16] and Bruemmer et al. [14].

alloy, shown in Fig. 2(f). Tests were performed at room temperature and each data point represents the average of two yield stress measurements and three hardness measurements.

Toloczko et al. [16] correlated Vickers hardness testing and uniaxial yield stress using tests on unirradiated 316 SS samples cold-worked to various levels, resulting in hardness ranging from 138 to 344 kg/mm^2. This data is illustrated in Fig. 2(f). Both hardness and yield stress were measured at room temperature. Again, the resulting correlation was linear in form and expressed as

$$\sigma_y = 2.7H_v - 125, \tag{9}$$

where σ_y is in MPa and H_v is in kg/mm^2. This relation is quite similar to that of Bruemmer et al., both in form and in magnitude of the coefficients.

3.2. Development of a correlation between hardness and yield stress

In order to develop a correlation using all of the data listed in the previous section, several factors must be considered. The dependence upon alloy composition (304 vs. 316) and test temperature (25 °C vs. 288 °C) is important. The form of the correlation is also important.

Clearly, yield stress and hardness are related in a linear fashion, as illustrated by the raw data in Fig. 2(a)–(f). However, the existing correlations discussed in the previous section vary somewhat in form. The relations developed by Tabor, Bruemmer et al., and Toloczko et al., are all based on the measured values of hardness and yield stress, while the relationship determined by Higgy and Hammad is based on the measured *changes* in hardness and yield stress. Both forms are useful.

The form chosen for this study is the change in yield stress vs. the change in hardness. This form is chosen for several reasons. First, by using the change in hardness and change in yield stress, one parameter is eliminated from the correlation (i.e. the y-intercept in Eqs. (8) and (9)). Further, a relationship using change in hardness or yield stress rather than absolute values is more applicable to all materials, regardless of the initial hardness or yield stress.

Hardness–yield stress correlation factors for the data (and subsets) from each author were calculated from change in hardness and change in yield stress and are listed in Table 1. The unirradiated hardness or yield stresses presented in each paper were used as the baseline values for determining the change in hardness and yield stress. The standard deviation, σ, associated with each correlation factor was also determined using standard methods for linear regression analysis [17,18]. Here, the standard deviation describes the amount of fluctuation expected in the calculated correlation factor. For a normal statistical distribution, there is a 95% probability that the "true" correlation factor lies within 2σ. The correlation factors calculated for the individual studies are also compared in Fig. 3, along with the error bars representing the 2σ calculated for each of the correlation factors. The standard deviations for the Furutani and Allen data are considerably larger than any of the other data sets, but this is likely due to a smaller number of data points than any other systematic error. Of significance

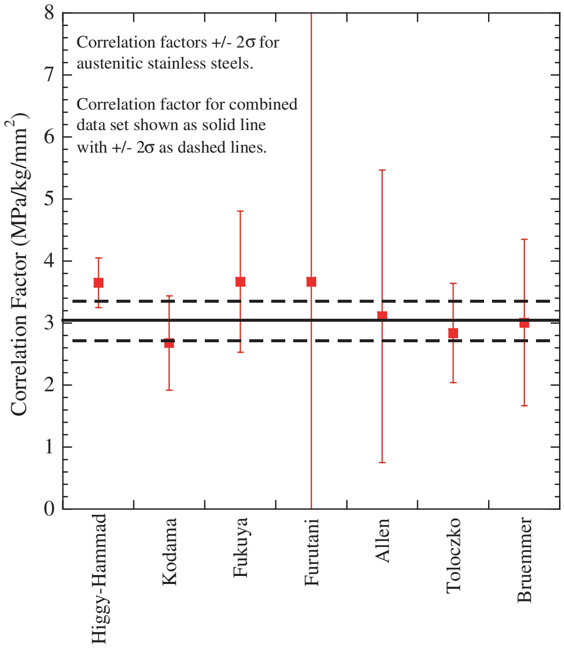

Fig. 3. Comparison of the correlation factors for each of the data sets used in this study. Also plotted are the 2σ values for the standard deviation associated with each calculated correlation factor.

Table 1
Comparison of correlation factors for austenitic stainless steels for the data sets used in this study and existing correlations

Study	Material	Hardness temperature (°C)	YS temperature (°C)	Correlation factor (MPa/kg/mm^2)[a]	Correlation factor uncertainty (MPa/kg/mm^2)[a]	R^2
Tabor[b]	Various	–	–	3.29	–	
Higgy and Hammad	304	25	25	3.76	0.21	0.99
	316	25	25	3.43	0.28	0.98
	347	25	25	3.55	0.49	0.96
	All	25	25	3.65	0.20	0.96
Kodama	304	25	288	3.06	2.78	0.99
	316	25	288	2.64	0.38	0.96
	347	25	288	2.63	3.05	0.95
	All	25	288	2.68	0.38	0.58
Fukuya	304	25	288	3.83	0.31	0.99
	316	25	288	3.58	0.78	0.96
	347	25	288	3.79	1.70	0.98
	All	25	288	3.67	0.57	0.58
Furutani	316	25	288	3.67	12.4	0.95
Allen	316	25	25	3.11	1.18	0.98
Toloczko	316	25	25	2.84	0.40	0.98
Bruemmer	316	25	25	3.01	0.67	0.98
All data	**316/304/347**	**25**	**25, 288**	***3.03***	***0.18***	**0.88**

[a] All correlation factors were converted to equivalent units.
[b] Theoretical study.

is that the correlation factors (and their associated error bars) for all the different studies overlap.

The change in yield stress from the measurements of all authors is plotted as a function of change in hardness in Fig. 4. Combined, the data covers a larger range of hardness and yield stress than any individual data set. Given the good agreement of correlation factors between the different studies, a single line was fit to the combined set using a least squares fit with the condition that the line passes through the origin. This line is also shown in Fig. 4. The resulting correlation between yield stress and hardness was determined to be

$$\Delta\sigma_y = 3.03\Delta H_v, \tag{10}$$

where $\Delta\sigma_y$ is expressed in MPa and ΔH_v is expressed in kg/mm^2, with an R^2 of 0.88. The standard deviation calculated for this correlation factor is 0.18 MPa/kg/mm^2, smaller than the standard deviation for any of the individual sets listed in Table 1 (due to the greater number of data points). The 95% confidence bounds were also determined using standard least squares techniques [17,18] and are shown in Fig. 4. The methodology for determining the standard deviation of the correlation factor and the 95% confidence bounds is highlighted in Appendix A. The confidence bounds shown in Fig. 4 define the region with a 95% probability of containing the true hardness–yield stress relation (but not necessarily the individual data points). That is, if the experiments were repeated, 95% of the correlations developed will lie within the confidence bounds. Note that the temperature dependence for change in hardness and yield stress measurements was assumed to be negligible. This assumption will be addressed in a following section.

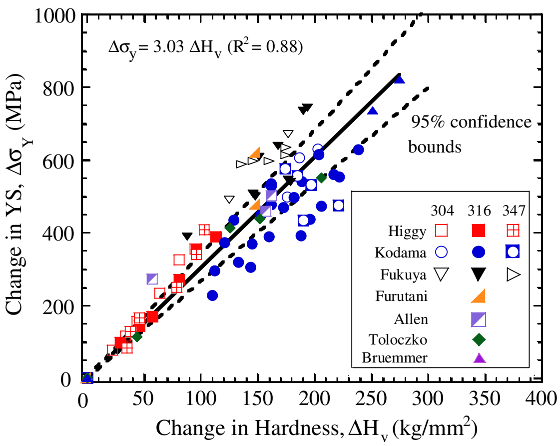

Fig. 4. All available experimental data plotted as a change in yield stress as a function of change in hardness for austenitic stainless steels. The hardness–yield stress correlation is also plotted along with 95% confidence bounds.

The correlation factor determined from the combined data set is compared to the existing correlations in Table 1 and Fig. 3. As this result is based upon the entire data set, it is not surprising that it lies in the middle of the previously reported values. Since the least squares fit was forced through the origin, it follows that the best fit for the combined data set must be an average of the fits for the individual data sets (weighted by the number of data in each individual set). While the fit to the entire data set is quite good (as evidenced by $R^2 = 0.88$ and $\sigma = 0.18$ MPa/kg/mm^2), other factors should be evaluated.

3.3. Composition and temperature dependence

Higgy and Hammad found that the correlation factors for 304, 316, and 347 were slightly different. However, as illustrated by the data in Fig. 4 and Table 1, no systematic difference exists between 304, 316, and 347 stainless steels. Indeed, the correlation factors and associated standard deviations for 304, 316, and 347 are similar, as shown in Table 1. The different alloy series examined by Kodama and Fukuya do show a larger variation than that by Higgy and Hammad. However, it is again important to note that the data from Kodama represent a single specimen, as opposed to the multiple samples tested by Higgy and Hammad. Further, the 304, 316, and 347 series by Kodama and Fukuya are composed of 39 different heats. These two factors may explain the larger scatter between alloys.

The temperature dependence of the change in yield strength was assumed to be negligible. Hardness and yield stress decrease with increasing temperature. However, the change in hardness or yield stress is unchanged with test temperature. Bruemmer et al. [14], demonstrated this to be true for hardness measurements on commercial purity 304 and 316 samples tested over a range of temperatures (room temperature up to 288 °C). Nunes and Larson [19] verified experimentally and theoretically that the correlation between hardness and yield stress is unchanged over a range of test temperatures (−196 °C to 200 °C) for a variety of metals (including mild steels, iron, copper, aluminum, and titanium). Therefore, the correlations shown in Fig. 3 and Table 1 should be valid, irrespective of the temperatures used for hardness and yield stress measurement.

3.4. Work-softening under irradiation

The influence of irradiation on work hardening under irradiation must also be considered. As shown by Byun et al. [20], the work-hardening exponent for 316 stainless steel decreased steadily with irradiation dose from the unirradiated value of 0.4 to a value of 0.1 by about 4 dpa. Such a change may also influence a hardness–yield stress correlation.

While yield stresses are measured at approximately 0.2% strain, hardness measurements represent material properties at much higher strains (8% as estimated by Tabor [5] up to 18% as modeled by Larsson [8]). Since the hardness measurements are taken at significant plastic strain, strain hardening effects must be considered. For a strain hardening exponent (n) greater than 0, and following irradiation where n changes, the correlation factor between yield strength and hardness (e.g. Eq. (10)) will also change. Following irradiation to a low dose (φ_1), there is an increase from the unirradiated condition for both yield stress ($\Delta\sigma_{y1}$) and stress calculated from hardness (ΔH_1). Irradiation to a higher dose (φ_2), results in a yield stress, σ_{y2} that is $\Delta\sigma_{y2}$ greater than σ_{y1}, and a hardness H_2 that is ΔH_2 greater than H_1, along with a corresponding decrease in n. For the case where $\Delta\sigma_{y1} = \Delta\sigma_{y2}$, ΔH_2 must be less than ΔH_1 due to the decrease in the strain hardening coefficient with dose. The ratio, $\Delta\sigma_y/\Delta\sigma_H$ is directly related to the correlation factor, and in this case, $\Delta\sigma_{y1}/\Delta H_1$ is less than $\Delta\sigma_{y2}/\Delta H_2$. Thus, as irradiation dose increases, the correlation factor between $\Delta\sigma_y$ and ΔH_v also increases.

Examination of the data in Fig. 3 suggests that such an effect may be important. In Fig. 5, the data set is separated into low hardening/dose (<100 kg/mm^2) and high hardening/dose (>100 kg/mm^2) regimes and a correlation found for each subset. The break-point was chosen at 100 kg/mm^2 as this is the hardness level that corresponds to the dose where the most significant change in work hardening was observed by Byun et al. [20] (∼3 dpa). For this two-part correlation, hardness and yield stress can be related as

$$\Delta\sigma_y = 3.63\Delta H_v \quad \text{for } \Delta H_v < 100\,\text{kg/mm}^2, \tag{11a}$$

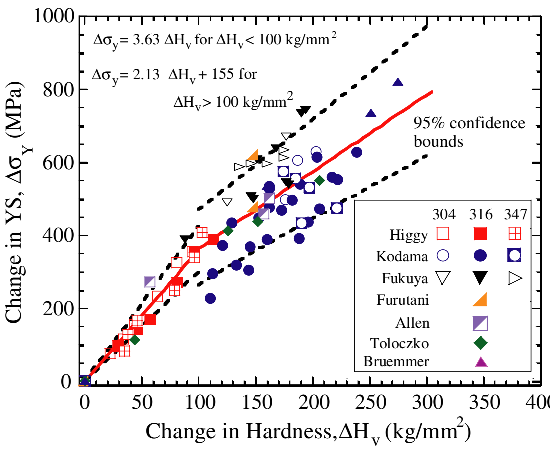

Fig. 5. Two-part correlation between change in hardness and change in yield stress for all available experimental data. The hardness–yield stress correlation is also plotted along with 95% confidence bounds.

$$\Delta\sigma_y = 2.13\Delta H_v + 155 \quad \text{for } \Delta H_v > 100\,\text{kg/mm}^2. \tag{11b}$$

The two-part correlation is plotted in Fig. 5, along with the 95% confidence bounds. The standard deviation of the correlation factors for the first and second portion of the correlation are 0.25 and 0.34, respectively, while the standard deviation calculated for the y-intercept in Eq. (11a) is 59 MPa. For Eq. (11b), the correlation factor of 3.63 ($R^2 = 0.92$) and associated standard deviations closely match that from Higgy and Hammad, which is expected as the bulk of the data below 100 kg/mm^2 is from that study. The correlation factor for the second portion of the correlation is considerably lower at 2.13, inconsistent with the expected work-softening effect as described above. Further, the R^2 for this portion of the correlation is only 0.41, while the uncertainty has increased to 0.34, indicating that the entire data set is better fit with a single linear fit. While work-softening may indeed be an important effect in understanding the relationship between microhardness measurements and yield stress in irradiated austenitic alloys more analysis is needed. Further, the current data set can be modeled more accurately without accounting for such effects.

3.5. Summary for austenitic alloys

The data points from seven individual studies have been combined in this study in order to formulate a correlation between change in measured hardness and change in measured yield stress for irradiated austenitic stainless steels. The combined data set spans a wider range of hardness, yield stress, alloy, irradiation and test conditions than any individual data set. Further, the correlation factors for data from the separate studies are similar and lie within 2σ of each other, as shown in Fig. 4. A correlation, independent of material composition or test temperature was found. The resulting correlation between change in yield stress and change in hardness, independent of alloy composition or temperature, was determined to be

$$\Delta\sigma_y = 3.03\Delta H_v,$$

where $\Delta\sigma_y$ is expressed in MPa and Δh_v is expressed in kg/mm^2.

The measured yield stress for each of the data points in this study are compared as a function of irradiation dose in Fig. 6(a) to an extensive set of yield stress measurements for irradiated austenitic stainless steels available in the open literature [21–26]. Plotted in Fig. 6(b) are the yield stresses calculated from hardness measurements using the correlation developed in this study. The calculated yield stress values from microhardness measurements used in this study are in good agreement with the measured yield stress values (from the same alloy/dose condition) for the data used in this study and that from the open literature.

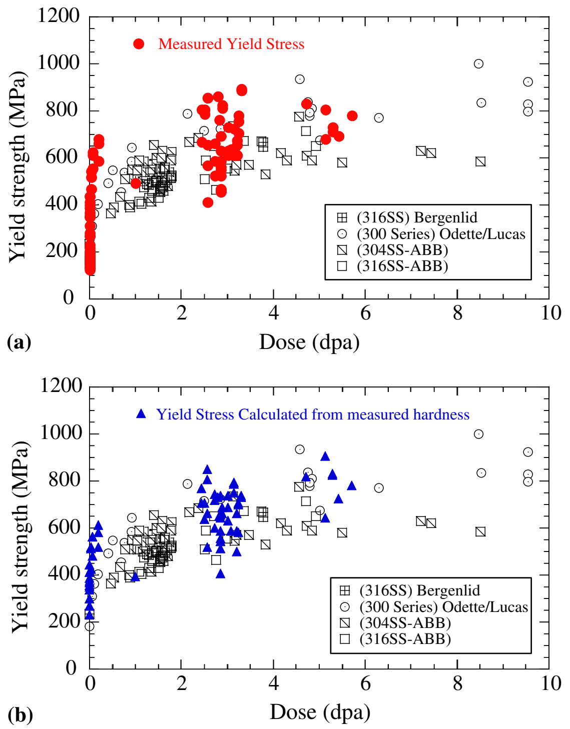

Fig. 6. (a) Comparison of measured yield stress from data used in this study and other data available in the open literature [21–26]. (b) Comparison of yield stress calculated from hardness data used in this study and other yield stress measurements available in the open literature.

4. Ferritic steels

The mechanical properties of ferritic steels used as reactor pressure vessels are also of great interest. Six sets of data [27–32] were identified in the open literature describing both the Vickers hardness and the yield strength of hardened ferritic steels. Each of these datasets will be presented by describing the materials included in the study, the measured physical properties, and the method by which these properties were determined. The data sets are combined and a single correlation between hardness and yield stress is developed following the same methodology used for the austenitic steels.

4.1. Existing correlations and data

A particularly extensive tabulation of yield stress and hardness for ferritic steels is given in the ASM Handbook, volume 8, Mechanical Testing and Evaluation [27]. The ASM Handbook presents data from a set of carbon and low alloy steels in annealed, normalized, and quenched and tempered states. Hardness was measured at room temperature with a 1.0 kg load. The complete data set covers a range in increase of hardness up to 560 kg/mm^2. However, for the purposes of this study, only data up to an increase in hardness of 100 kg/mm^2 will be used as hardness increases in neutron-irradiated ferritic steels are typically less than this value. Therefore, to provide a correlation that is most relevant to RPV steels, the ASM dataset will be limited to a change in hardness of less than 100 kg/mm^2. The data set is shown in Fig. 7(a) and exhibits a highly linear fit with an R^2 of 0.99. A correlation factor of 3.12 was calculated for this set with a standard deviation of 0.06 MPa/kg/mm^2 (see Table 2).

Mancuso et al. [28] studied the correlations between microhardness, tensile properties, and notch ductility of ferritic steels irradiated with neutrons to various doses at 288 °C. The ferritic alloys had small differences in bulk Cu content (0.23–0.28 wt%). The hardness and yield strength measurements are illustrated in Fig. 7(b) and the correlation factor and standard deviations are listed in Table 2.

A third such comparison can be found in a publication by Lucas et al. [29]. In this study the hardness/yield strength relationship was considered for lightly irradiated materials (pure metals, pressure vessel steels, high alloy steels). Fig. 7(c) represents the data provided comparing the change in Vickers hardness and yield strength. The scatter in the Lucas data is greater than that shown for the ASM compilation and that of Mancuso, with an R^2 of only 0.77, although the standard deviation of the correlation factor for the Lucas data is smaller than that for Mancuso, likely due to the greater number of data points.

Gorynin et al. [30] measured Vickers hardness and yield strength data in neutron-irradiated reactor pressure vessel steels. The samples were irradiated at 250 °C to 3×10^{23} n/m^2 and are well represented by a linear fit (correlation factor of 2.87 and R^2 of 0.95) The resulting data are shown in Fig. 7(d).

Work by Jones et al. [31] on a neutron-irradiated (240 °C for 100 days in Halden reactor) steel showed a change of Vickers hardness of 15.40 kg/mm^2 corresponding to a change in yield strength of 12.50 MPa. This study only included the one set of hardness and yield strength data. Finally, Suzuki et al. [32] measured the relationship between Vickers hardness and yield strength for pure iron and low alloy steels irradiated at 260–275 °C. Suzuki reports only two data points. The Jones and Suzuki data are plotted together in Fig. 7(e) and are included in the final assessment.

4.2. Development of a correlation between hardness and yield stress for ferritic steels

The data for the ferritic steels are summarized in Table 2 and Fig. 8. All of the data described above have been combined into a single plot; Fig. 9. The correlation

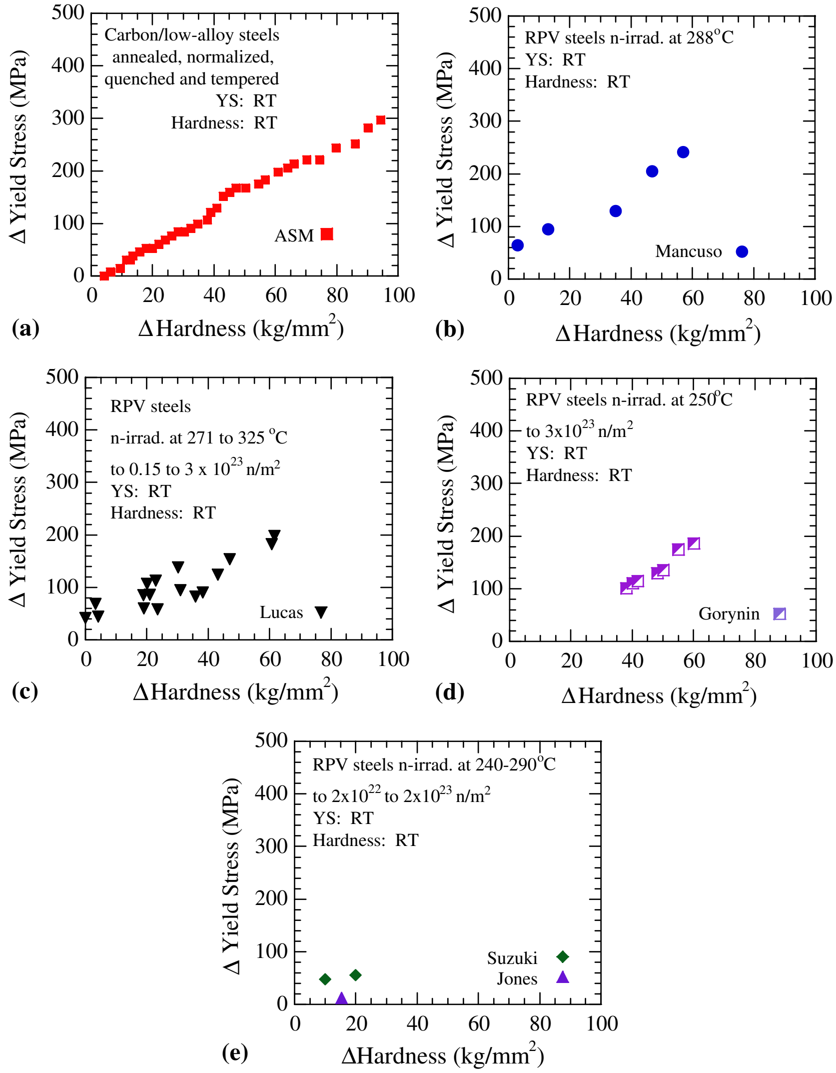

Fig. 7. Available experimental data comparing yield stress and hardness in ferritic reactor pressure vessel steels. Data taken from (a) ASM [27], (b) Mancuso et al. [28], (c) Lucas et al. [29], (d) Gorynin et al. [30], and (e) Jones et al. [31] and Suzuki et al. [32].

Table 2
Comparison of correlation factors for ferritic steels for the individual data sets of this study

Study	Material	Hardness temperature (°C)	YS temperature (°C)	Correlation factor (MPa/kg/mm^2)[a]	Correlation factor uncertainty (MPa/kg/mm^2)[a]	R^2
ASM[b]	Carbon and low alloy steels	25	25	3.12	0.06	0.99
Mancuso	RPV Steels	25	25	4.28	0.86	0.94
Lucas	RPV Steels	25	25	3.20	0.43	0.77
Gorynin	RPV Steels	25	25	2.87	0.61	0.95
All data	–	**25**	**25**	***3.06***	***0.15***	**0.90**

[a] All correlation factors were converted to equivalent units.
[b] Only data for ΔH_v <100 kg/mm^2 used in formulation of correlation.

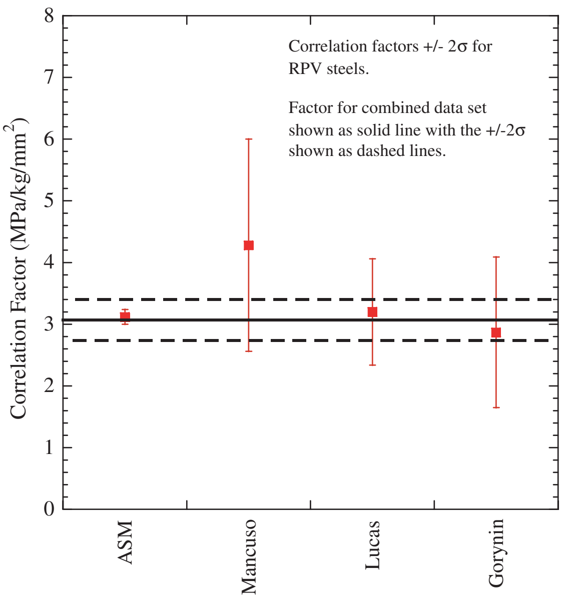

Fig. 8. Comparison of the correlation factors for each of the ferritic steel data sets used in this study. Also plotted are the 2σ values for the standard deviation calculated for each correlation factor.

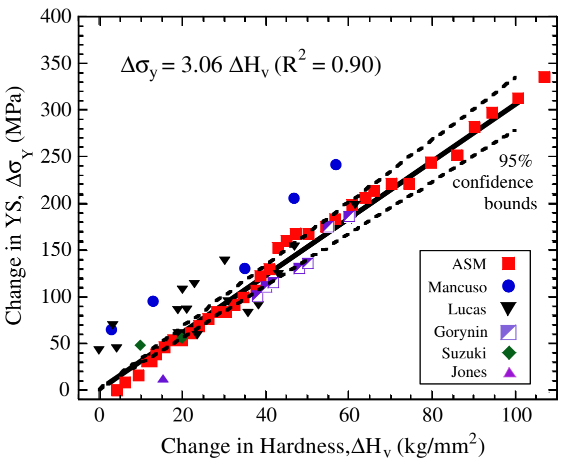

Fig. 9. All available experimental data plotted as a change in yield stress as a function of change in hardness for ferritic stainless steels. The hardness–yield stress correlation is also plotted along with 95% confidence bounds.

factors for the ferritic steels are in good agreement, with each factor lying within the 2σ bars of the factors of the other studies. As with the austenitic alloys, a linear fit was applied to the combined data set. The combined data set spans a wider range of hardness, yield stresses, allloys, irradiation, and test conditions than any individual data set and the data from the separate studies. The resulting correlation between change in yield stress and change in hardness was determined to be

$$\Delta\sigma_y = 3.06\Delta H_v, \quad (12)$$

where $\Delta\sigma_y$ is expressed in MPa and ΔH_v is expressed in kg/mm^2. For this correlation, the R^2 was found to be 0.90 and the standard deviation of the correlation factor is 0.15. As illustrated in Fig. 8, the correlation factors for three of the four data sets lie within the 2σ boundary.

5. Comparison of correlations for austenitic and ferritic steels

It is also informative to compare the correlations determined for the austenitic and ferritic steels. The correlation factors for the austenitic and ferritic steels were virtually the same at 3.03 and 3.06 MPa/kg/mm^2, respectively. That the results for the two alloy systems are so similar is somewhat surprising given the distinct differences in crystal structure, material properties, and typical operating conditions. However, Tabor's original theoretical derivation predicted a correlation factor of 3.33 MPa/kg/mm^2, *independent* of alloy type or structure. This is also supported by Tabor's own experimental results [5] where he found that the correlation factors for mild steel and annealed copper were very similar (3.44 and 3.33, respectively), consistent with the results of this study.

6. Conclusions

The relationship between yield stress and hardness measurements has been examined for both irradiated austenitic and ferritic steels and a correlation for each alloy system has been developed. For irradiated austenitic stainless steels, the data from seven separate studies have been merged. The combined data set covers 304, 316, and 347 stainless steels irradiated with neutrons (to various doses at various temperatures) or cold worked to different levels. The data from the separate studies are in excellent agreement with each other and a correlation, independent of material composition or test temperature was found. The resulting correlation between change in yield stress and change in hardness was determined to be

$$\Delta\sigma_y = 3.03\Delta H_v,$$

where $\Delta\sigma_y$ is expressed in MPa and ΔH_v is expressed in kg/mm^2.

For ferritic steels, data from six separate studies have been combined and a correlation between hardness and yield stress has been calculated. As with the austenitic alloys, the data from the separate studies are in excellent agreement with each other. The resulting correlation between change in yield stress and change in hardness for ferritic steels was determined to be

$$\Delta\sigma_y = 3.06\Delta H_v,$$

where $\Delta\sigma_y$ is expressed in MPa and ΔH_v is expressed in kg/mm^2.

Acknowledgment

The authors would like to thank Kjell Peterson for many useful and insightful discussions. Support at the University of Michigan was provided by Cooperative IASCC Research (CIR) program through EPRI contract EP-P3038/C1434.

Appendix A. Statistical methods

For each set of data, a correlation factor was calculated using least squares techniques. A standard deviation was also calculated for each correlation factor, along with 95% confidence bounds. The methodology for those calculations is presented below.

There are numerous ways to fit a straight line of the form $y = mx + b$ to a set of data. It is assumed that x is the independent variable and y is dependent. In the least-squares method, it is assumed that all scatter in the data points is due to errors in measuring y and that the best straight line is that which minimizes the sum of the squares of the errors, s_y^2, in the y-direction. More specifically,

$$s_y^2 = \frac{1}{n-2}\sum_{i=1}^{n}[y_i - (b + mx_i)]^2, \tag{A.1}$$

where n is the number of data points and x_i and y_i are the individual data pairs. When s_y^2 is minimized, m and b have been optimized and represent the best-fit line to the data. With information on s_y^2, the sample variance for b and m can also be determined using propagation of error techniques [17,18].

The uncertainty of the slope of the best-fit line can be calculated using the relation:

$$s_m^2 = \frac{ns_y^2}{d}, \tag{A.2}$$

where n is again the number of data points and d is

$$d = n\sum x^2 - \left(\sum x\right)^2. \tag{A.3}$$

While most of the correlations developed in this paper used a line forced through the origin ($b = 0$), the two-part correlation between hardness and yield stress also used an intercept. The uncertainty of the intercept of the line can be also be determined using

$$s_b^2 = \frac{s_y^2\sum x^2}{d}, \tag{A.4}$$

where d is calculated using Eq. (A.3).

The confidence bounds can be formulated using the Student's t-test approach. To perform the t-test, a level of significance, α, is chosen (for this study $\alpha = 0.05$ for a confidence bound of 95%). With this and the number of degrees of freedom (here, this is $n - 2$ as the data has been used to calculate m and b) we can obtain a critical t value, t_{cr}, by solving

$$(0.5 - \alpha/2) = \int_o^{t_{cr}} t(x)\mathrm{d}x, \tag{A.5}$$

where $t(x)$ is the student's t-point distribution function. The results of this integration are readily available in t-test tables. Using the degrees of freedom and the level of significance, t_{cr} can be determined. For example, for the austenitic steels, 133 data points were used. For $\alpha = 0.05$ and $n-2 = 131$, t_{cr} is 1.665.

Now, the confidence bounds are

$$\hat{y} = mx + b \pm t_{cr}s_{\hat{y}}, \tag{A.6}$$

where $s_{\hat{y}}$ is the variance evaluated at x, or,

$$s_{\hat{y}}^2 = s_m^2x^2 + s_b^2, \tag{A.7}$$

where s_m^2 and s_b^2 are determined from Eqs. (A.2) and (A.4), respectively. Combining Eqs. (A.6) and (A.7), the confidence bounds are

$$\hat{y} = mx + b \pm t_{cr}\sqrt{s_m^2x^2 + s_b^2}. \tag{A.8}$$

The plot of these equations is the contour curve shown, for example, in Fig. 4. These confidence bounds do not necessarily contain 95% of the individual data points. Rather, they define the region with a 95% probability of containing the true hardness–yield stress relation. That is, if the experiments were repeated, 95% of the correlations developed will lie within the confidence bounds.

References

[1] S.J. Zinkle, P.J. Maziasz, R.E. Stoller, J. Nucl. Mater. 206 (1993) 266.
[2] P.J. Maziasz, J. Nucl. Mater. 205 (1993) 118.
[3] G.E. Lucas, J. Nucl. Mater. 206 (1993) 287.
[4] G.S. Was, J.T. Busby, T.R. Allen, E.A. Kenik, A. Jenssen, S.M. Bruemmer, J. Gan, A.D. Edwards, P.M. Scott, P.L. Andresen, J. Nucl. Mater. 3000 (2002) 198.
[5] D. Tabor, Br. J. Appl. Phys 7 (1956) 159.
[6] L. Prandtl, Nachr. Ges. Wiss. Gottingen. (1920) 74.
[7] H. Hencky, Z. Agnew. Math. Mech. 3 (1923) 250.
[8] P.L. Larsson, Int. J. Mech. Sci. 43 (2001) 895.
[9] H.R. Higgy, F.H. Hammad, J. Nucl. Mater. 55 (1975) 177.
[10] M. Kodama, S. Suzuki, K. Nakata, S. Nishimura, K. Fukuya, T. Kato, Y. Tanaka, S. Shima, in: 8th International Symposium on Environmental Degredation-Water Reactors, 1997 August, p. 833.

[11] K. Fukuya, S. Shima, K. Nakata, S. Kasahara, A. Jacobs, G. Wozadlo, S. Suzuki, M. Kitamura, in: R.E. Gold, E.P. Simonen (Eds.), 6th Environmental Degradation, TMS, 1993.
[12] G. Furutani, N. Nakajima, T. Konishi, M. Kodama, J. Nucl. Mater. 288 (2001) 179.
[13] T.R. Allen, H. Tsai, J.I. Cole, J. Ohta, K. Dohi, H. Kusanagi, in: M.L. Grossbeck, T.R. Allen, R.G. Lott, A.S. Kumar (Eds.), Effects of Radiation on Materials: 21st International Symposium, ASTM STP 1447, ASTM International, West Conshohocken, PA, 2003.
[14] S.M. Bruemmer et al., Characterization of Neutron-Irradiated 300-Series Stainless Steels to Assess Mechanisms of Irradiation Assisted Stress Corrosion Cracking, Final Report, EPRI Project WO4068-20, November 2000.
[15] S. Suzuki, Y. Tanaka, M. Kodama, S. Nishimura, K. Fukuya, S. Shima, K. Nakata, T. Kato, Mechanical Properties and SSRT results of various kings of irradiated stainless steels, Presented at 12th ICG-IASCC meeting, Toronto, Canada, April 1996.
[16] M.B. Toloczko et al., in: 17th International Symposium on Effects of Rad. On Materials, STP1270, 1996, p. 902.
[17] L. Lyons, Statistics for Nuclear and Particle Physicists, Cambridge University, 1989, p. 125.
[18] N.D. Eckhoff, Principles of Engineering Analysis, vol. II, Kansas State University, 1993, p. 6.
[19] J. Nunes, F.R. Larson, J. Inst. Met. 91 (1962-63) 114.
[20] T.S. Byun, K. Farrell, E.H. Lee, J.D. Hunn, L.K. Mansur, J. Nucl. Mater. 298 (2001) 269.
[21] G.S. Was, Use of Proton Irradiation to Understand IASCC in LWR's, Final Report, EPRI, RP4068-26, 2001.
[22] S.M. Bruemmer, et al., Characterization of Neutron-Irradiated 300-Series Stainless Steels to Assess Mechanisms of Irradiation Assisted Stress Corrosion Cracking, Final Report, EPRI Project WO4068-20, November 2000.
[23] G.R. Odette, G.E. Lucas, J. Nucl. Mater. 179–181 (1991) 572.
[24] Bergenlid, U., Haag, Y., K. Pettersson, The Studsvik MAT 1 Experiment. R2 Irradiations and Post-Irradiation Tensile Test, Studsvik Report STUDSVIK/NS-90/13, Studsvik Nuclear, 1990.
[25] A. Jenssen, Written communication, 1998.
[26] G.R. Odette, G.E. Lucas, Fusion Reactor Materials-Semiannual Progress Report for Period Ending 31 March 1989, US Department of Energy, DOE/ER-0313/6, 1989 313.
[27] Kuhn H., Medlin D. (Eds.), American Society for Metals Handbook, vol. 8, American Society for Metals, 2000, p. 273.
[28] J.F. Mancuso, J.A. Spitznagel, R.P. Shogan, J.R. Holland, in: D. Kramer, H.R. Brager, J.S. Perrin (Eds.), Effects of Radiation on Materials: Tenth Conference, ASTM STP 725, American Society for Testing and Materials, 1981, p. 38.
[29] G.E. Lucas, G.R. Odette, R. Maiti, J.W. Sheckherd, in: Influence of Radiation on Material Properties: 13th International Symposium, Part II, ASTM STP 956, American Society for Testing and Materials, 1987, p. 379.
[30] I.V. Gorynin, E.V. Nesterova, V.A. Nikolaev, V.R. Rybin, in: Effects of Radiation on Materials: 17th International Symposium, ASTM STP 1270, American Society for Testing and Materials, 1996, p. 248.
[31] R.B. Jones, J.R. Cowan, R.C. Corcoran, J.C. Walmsley, in: Effects of Radiation on Materials: 19th International Symposium, ASTM STP 1366, American Society for Testing and Materials, 2000, p. 473.
[32] M. Suzuki, K. Onizawa, M. Kizaki, in: Effects of Radiation on Materials: 17th International Symposium, ASTM STP 1270, American Society for Testing and Materials, 1996, p. 351.